ASTRO SCIENCES

FINAL REPORT

ON CONTRACT NASW-1863-Mod 1

SPECTROSCOPIC OBSERVATIONS OF THE PLANETS

IITRI
IIT RESEARCH INSTITUTE
10 West 35 Street
Chicago, Illinois 60616

FINAL REPORT

ON CONTRACT NASW-1863-Mod 1

SPECTROSCOPIC OBSERVATIONS OF THE PLANETS

by

A. B. Binder

Astro Sciences
IIT Research Institute
Chicago, Illinois 60616

for

Dr. William E. Brunk
Chief of Astronomy, Code SL
NASA Planetary Programs Div., FOB 6
Washington, D. C. 20546

Contract No. NASW-1863-Mod 1

Respectfully submitted,
IIT Research Institute

D K Roberts

for Alan B. Binder
Research Scientist

APPROVED BY:

C A Stone

C. A. Stone, Director
Physics Division

SUMMARY

This final report on Project NASW-1863-Mod 1 contains a description of the results obtained principally from a series of 10 channel IR spectrophotometer observations of the 1.5 μm window of Jupiter. These results show that the NH_3 and CH_4 absorptions increase with increasing air mass along N-S traces taken at the central meridian of Jupiter and decrease with increasing air mass along E-W traces taken along the Jovian belts and zones. These variations in the absorptions over the disk indicate that the NH_3 and CH_4 bands are being formed in a scattering atmosphere rather than an atmosphere with a simple reflecting cloud layer. The results also show that the absorptions over the South Tropical Zone are considerably greater than for the rest of the features at equivalent air mass while the absorptions over the Great Red Spot are considerably less than for other features.

The data were also used to show that the Minnaert function can be used to describe the limb darkening of Jupiter, at least at 1.5 μm, and that the scattering layer probably behaves like a Lambertian surface.

Some preliminary observations of Titan in the 6000 Å - 2.3 μm region and 10 channel data programs for Jupiter/Saturn and point objects are briefly discussed.

TABLE OF CONTENTS

CAPTIONS

Figure 1. The spectrum of Jupiter between 1.35 and 1.65 μm according to Cruikshank and Binder (1968, 1969). The bars superimposed on the spectrum indicate the equivalent wavelength passbands of the first eight cells of the 10 channel spectrophotometer. Due to strong CH_4 absorptions, Jupiter is essentially black for several tenths of a μm beyond 1.65 μm. As a result, the passbands for the ninth and tenth cells, which are centered at 1.67 and 1.70 μm respectively, are not shown.

Figure 2. Schematic representation of Jupiter as it appeared during April-June, 1970. The circles superimposed on the various features indicate the relative size and positions of the areas observed with the 10 channel spectrophotometer. The observations of the GRS and LWO's (shown on the north edge and the south edge of the STB respectively) were made at the centers of these spots when they were at a variety of distances from the CM.

Figure 3a. Percent absorption of NH_3 as a function of Jovian air mass for the points observed on a N-S trace along the CM. The percent absorption was computed using the data obtained from the 1.47, 1.50 and 1.53 μm passband cells (see Table 1). The filled circles represent the data for belts and polar regions. The open circles represent the data for the zones. The STrZ (at 2.05 AM) and the EZ (at 2.00 AM) lie above the curve defined by the dark

features while the NTrZ (at 2.35 AM) may fall on the dark feature curve.

Figure 3b. Percent absorption of NH_3 as a function of Jovian air mass for the points observed on a N-S trace along the CM. The percent absorption was computed using the data obtained from the 1.50 and 1.53 μm passband cells only (see Table 1). Otherwise, same as Figure 3a.

Figure 4. Percent absorption of NH_3 as a function of Jovian air mass for points observed along individual belts, zones, or following a spot across the disk. The percent absorption was computed using the data obtained from the 1.47, 1.50 and 1.53 μm passband cells (see Table 1).

Figure 5. Percent absorption of NH_3 as a function of Jovian air mass for points observed along individual belts, zones, or following a spot across the disk. The percent absorption was computed using the data obtained from the 1.47, 1.50 and 1.53 μm passband cells (see Table 1).

Figure 6. 1.5 μm NH_3 absorption map for the period April - June, 1970. The contours are in percent absorption as computed using the data obtained from the 1.47, 1.50 and 1.53 μm passband cells (see Table 1).

Figure 7. Percent absorption of CH_4 as a function of Jovian air mass for points observed on a N-S trace along the CM (see Table 1).

Figure 8. Percent absorption of CH_4 as a function of Jovian air mass for points observed along individual belts, zones or following a spot across the disk (see Table 1).

FINAL REPORT
CONTRACT NASW-1863-Mod 1

SPECTROSCOPIC OBSERVATIONS OF THE PLANETS

1. INTRODUCTION

During the period of performance on Contract NASW-1863-Mod 1 (V6097) a very successful series of observational runs were made on Jupiter, runs which have provided new data on the Jovian photometric function and on the distribution of the NH_3 and CH_4 over the disk of the planet. Additional series of observational runs were attempted in order to obtain colorimetric data on Jupiter, Saturn, Saturn's rings, Uranus, Neptune and the brighter satellites of the Jovian planets. However, exceptionally bad weather prevailed during these runs, and as a result only a few preliminary sets of data were obtained.

In addition to the observational and data interpretation activities carried out on Contract NASW-1863-Mod 1 (V6097), 10 channel data reduction programs were developed for Jupiter/Saturn and point objects (i.e., satellites, Uranus, and Neptune).

A detailed discussion of the observational runs, the results obtained from the observations, and data reduction programs are given in the following sections.

2. OBSERVATIONAL RUNS

The observations made during this program were carried out with the IITRI 10 channel IR spectrophotometer at the Lunar and Planetary Laboratory's Catalina Observatory, the McDonald Observatory, and the Kitt Peak National Observatory.

The Catalina observations were made with the 61" reflector and were carried out on 6 out of 12 assigned nights between April 3, and June 15, 1970 (6 nights were cloudy). During this period, 86 sets of 2.3" resolution (~ 1/20 the apparent diameter of Jupiter) measurements were made of the 1.5 μm window where the NH_3 absorptions have been shown to show disk positional and perhaps time dependent variations (Moroz and Cruikshank, 1969). The spectral resolution was 300 Å/cell and the wavelength range observed was 1.40 - 1.70 μm (see Figure 1). As is schematically shown in Figure 2, the data were taken on the CM (Central Meridian), near the evening and morning limbs (or terminator) and halfway between the CM and the morning and evening limbs for the NPR_s (North Polar Region, south edge), NTrZ (North Tropical Zone), NEB (North Equatorial Belt), EZ (Equatorial Zone), STrZ (South Tropical Zone), STB (South Temperate Belt), and the SPR_n (South Polar Region, north edge). Measurements were also made of the GRS (Great Red Spot) and the LWO's (Long Enduring White Ovals) at a variety of distances from the CM, the SEB (South Equatorial Belt) on the CM and the NPR and SPR near the respective poles.

The McDonald runs were made with the 82" reflector and covered the periods of November 7-12, 1970, and December 15-20, 1970. The purpose of these runs was to obtain colorimetric data ($\lambda\lambda$ 6000 Å - 2.3 μm, $\Delta\lambda$ ~ 1000 Å) on Saturn, Saturn's rings, the brighter satellites of Saturn, and Uranus. Exceptionally poor weather prevailed during both runs and only a few,

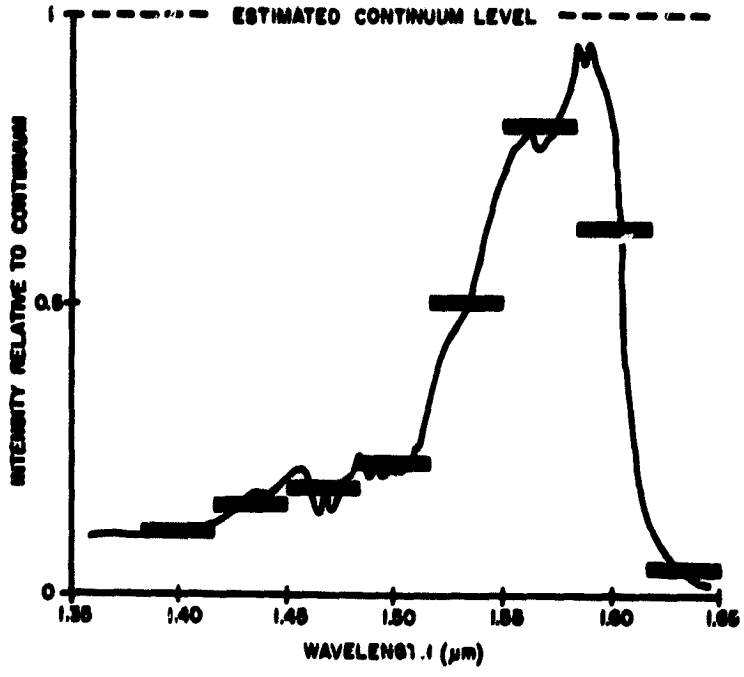

FIGURE 1 The spectrum of Jupiter between 1.35 and 1.65 μm according to Cruikshank and Binder (1968, 1969). The bars superimposed on the sprectrum indicate the equivalent wavelength passbands of the first eight cells of the 10 channel spectrophotometer. Due to strong CH_4 absorptions, Jupiter is essentially black for several tenths of a μm beyond 1.65 μm. As a result, the passbands for the ninth and tenth cells, which are centered at 1.67 and 1.70 μm respectively, are not shown.

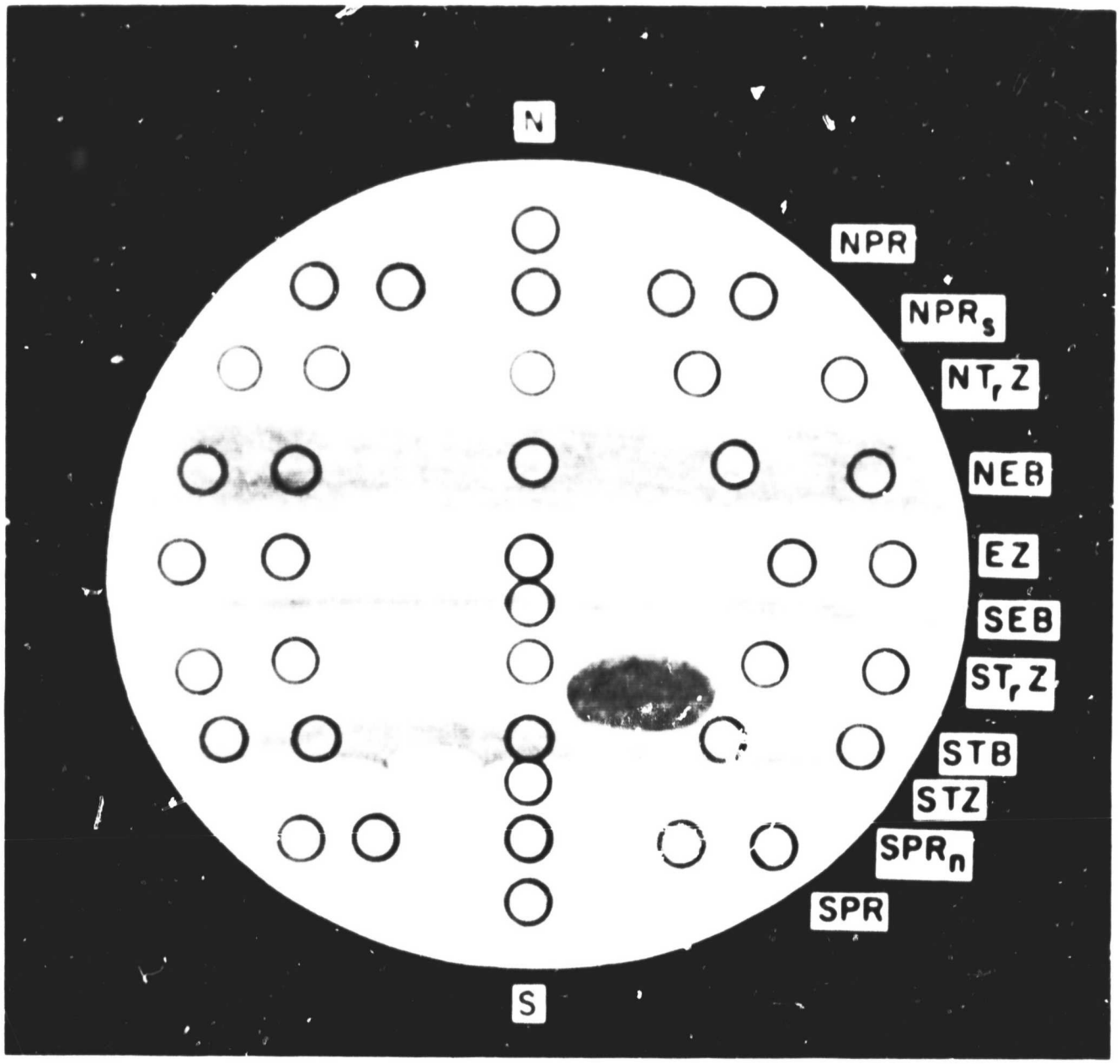

FIGURE 2 Schematic representation of Jupiter as it appeared during April-June, 1970. The circles superimposed on the various features indicate the relative size and positions of the areas observed with the 10 channel spectrophotometer. The observations of the GRS and LWO's (shown on the north edge and the south edge of the STB respectively) were made at the centers of these spots when they were at a variety of distances from the CM.

preliminary sets of data were obtained under very poor observational conditions. However, the data obtained on Titan represent the first 1-2.5 μm observations of this object and as such are of value despite their preliminary nature.

The final run was carried out on May 9-11, 1971 using the 50" reflector at KPNO. The purpose of this run was to obtain colorimetric data ($\lambda\lambda$ 6000 Å - 2.3 μm, $\Delta\lambda \sim$ 1000 Å) on Jupiter, the Galilean satellites, Uranus and Neptune. Poor seeing and clouds limited the observing time to about 1 hour during which 16 sets of 2".8 resolution measurements were made of Jupiter.

3. THE 1.5 μm JUPITER DATA

The data acquired on the 1.5 μm window of Jupiter has provided more extensive data and much more complete coverage (see Table 1 of Moroz and Cruikshank) at higher resolution (6 times the highest areal resolution obtained by Moroz and Cruikshank) than hitherto available on the NH_3 and CH_4 distribution over the disk of Jupiter as defined by the 1.5 μm bands. They also have provided an empirical definition of the limb darkening of Jupiter in the 1.5 μm region, and, as a result, provided new information which will be of use in the theoretical analysis of the structure of the Jovian atmosphere and the analysis of the thermal balance of the planet.

3.1. THE DISTRIBUTION OF NH_3 OVER THE DISK OF JUPITER

The spectrophotometric measurements of the 1.5 μm window provided measurements of the percent absorption of the combination of the overlapping 1.51 and 1.53 μm strong bands of NH_3. Because the 10 channel does not provide a continuous spectrum, it is impossible to obtain the equivalent widths of

the absorption bands. As a result, the measurements are discussed in terms of the percent absorption as indirectly measured by those cells whose equivalent passbands lie within the spectral region of the bands.

According to Jovian and laboratory spectra (Kuiper, 1964; Cruikshank and Binder, 1968, 1969) these 1.51 and 1.53 μm bands extend from about 1.45 μm to 1.56 μm. Thus the 1.47, 1.50, and 1.53 μm passband cells cover the region of interest and provided the data needed to measure the total absorption of the bands. However, the 1.44 μm CH_4 band overlaps the 1.45 μm cell. As a result, computations of the NH_3 absorptions were made using the data from the 1.50 and 1.53 μm cells only, and then using the data from the 1.47, 1.50 and 1.53 μm cells in order to evaluate the effects of the overlapping CH_4 bands on the results.

The continuum level, which is needed in order to compute the percent of absorption, is difficult to define in this spectral region because no part of the region is completely free of NH_3 or CH_4 bands or their wings. However, the continuum level cannot be far above the maximum of 1.58 μm (see Figure 1) since a solar line has been identified at the peak (Cruikshank and Binder, 1968, 1969). Because of its proximity to the peak at 1.58 μm, the 1.57 μm cell was used to estimate the continuum level even though the passband of this cell lies within the relatively weak 1.57 μm NH_3 band and the wing of the 1.53 μm NH_3 band. While this procedure precludes the determination of the absolute percent absorption, it does provide an accurate relative measurement of the absorptions. Table 1 gives the listing of the NH_3 absorption measurements versus disk position and Jovian air mass (AM).

TABLE 1

PERCENT ABSORPTION OF THE 1.5 μm AMMONIA AND METHANE BANDS AT DIFFERENT POSITIONS ON THE DISK OF JUPITER

FEATURE[a]	LATITUDE (DEG.)	AIR MASS	AM ERROR	PERCENT ABSORPTION AND ERROR (Δ) FOR					
				NH_3[b]	Δ	NH_3[c]	Δ	CH_4[d]	Δ
NPR, CM	+56.2	3.91	0.28	77	13	73	15	91	12
CM	+56.6	3.96	0.29	79	11	73	10	92	11
NPR_s, CM	+40.2	2.75	0.09	74	8	72	10	88	6
CM	+40.7	3.04	0.13	80[e]	6	74[e]	5	96[e]	5
CM	+43.5	2.92	0.11	72	4	67	3	85	3
M	+43.8	3.46	0.18	69	7	62	6	79[e]	7
E	+44.1	3.28	0.17	70	16	64	16	86	19
ML	+42.6	4.41	0.37	64	5	56	4	85	7
EL	+43.1	4.05	0.35	66	15	57	15	85	17
NTrZ, CM	+28.9	2.35	0.05	69	10	64	10	86	11
CM	+27.9	2.33	0.05	70	9	63	8	86	10
CM	+28.2	2.34	0.05	71	7	66	6	83	7
CM	+28.7	2.36	0.11	70	4	63	2	85	3
CM	+30.0	2.39	0.05	68	4	62	2	81	3
M	+28.4	2.81	0.19	65	6	59	5	80	6
E	+28.7	2.69	0.18	67	4	61	3	83	3
ML	+27.8	4.53	0.84	57	5	48	4	78	5
EL	+28.6	4.17	0.77	60	16	53	15	72	18
NEB, CM	+14.7	2.10	0.02	60	6	56	5	77	6
CM	+14.1	2.09	0.02	59	9	53	8	76	10
CM	+15.6	2.11	0.03	63	5	57	4	79	4
CM	+16.6	2.13	0.03	64	27[e]	58	3	79	3
CM	+16.6	2.13	0.06	61	3	55	18	76	2
CM	+15.5	2.10	0.03	62	4	56	2	80	3
CM	+16.3	2.13	0.03	61	5	54	4	76	5
M	+16.3	2.54	0.07	56	5	50	5	73	5
E	+16.7	2.42	0.06	58	4	52	3	73	4
ML	+16.0	4.31	0.36	46	28[e]	41	28[e]	65	33[e]
EL	+16.8	4.08	0.36	52	5	46	4	67	4
EZ, CM	-0.7	2.00	0.01	60	7	54	6	75	6
CM	-1.7	2.00	0.01	62	4	55	3	76	3
CM	-1.4	2.00	0.01	61	5	56	5	76	5
CM	+3.7	2.02	0.01	61	6	55	5	77	6

TABLE 1 contd.

FEATURE[a]	LATITUDE (DEG.)	AIR MASS AM	ERROR	PERCENT ABSORPTION AND ERROR (Δ) FOR NH_3[b]	Δ	NH_3[c]	Δ	CH_4[d]	Δ
M	-2.0	2.28	0.04	59	4	53	2	75	2
E	-1.8	2.33	0.05	57	5	50	4	76	4
ML	-1.5	3.51	0.20	53	4	45	4	73	4
EL	-1.2	3.82	0.27	51	5	45	4	73	6
SEB,CM	-4.3	2.01	0.01	61	5	55	4	77	5
STrZ,CM	-15.3	2.04	0.02	72	9	66	8	89[e]	9
CM	-14.7	2.04	0.02	68	5	62	4	79	4
CM	-14.4	2.04	0.02	70	6	65	5	83	6
CM	-14.1	2.04	0.02	69	5	64	4	81	5
CM	-14.7	2.04	0.04	69	3	63	2	81	2
CM	-14.6	2.04	0.04	70	3	64	1	83	2
CM	-14.4	2.04	0.04	69	4	63	3	81	3
CM	-13.4	2.04	0.03	70	4	63	2	84	3
CM	-14.7	2.04	0.02	70	4	63	2	84	2
CM	-14.7	2.04	0.02	70	4	62	2	84	3
CM	-14.4	2.05	0.02	69	4	63	3	83	3
CM	-14.0	2.05	0.02	68	4	61	2	82	2
CM	-13.6	2.04	0.02	70	7	63	7	83	7
M	-14.4	2.40	0.05	67	11	61	11	83	12
E	-14.2	2.29	0.05	66	5	61	4	79	4
ML	-15.4	3.83	0.25	55	5	49	4	71	7
EL	-15.1	3.42	0.20	57	6	50	5	74	6
STB,CM	-27.2	2.20	0.04	67	6	61	6	83	6
CM	-27.4	2.20	0.04	65	4	58	2	82	2
CM	-27.4	2.20	0.04	66	4	59	3	82	4
M	-27.7	2.55	0.07	64	4	57	3	83	3
E	-27.5	2.48	0.07	62	7	55	6	80	6
ML	-27.6	3.66	0.22	58	5	50	4	81	4
EL	-27.3	3.76	0.22	53	3	46	2	76	2
STZ,CM	-35.6	2.38	0.06	72	5	66	3	84	4
SPRn,CM	-49.1	2.88	0.11	71	15	66	15	79[e]	16
CM	-42.6	2.60	0.15	74	5	68	4	89	5
M	-42.3	2.93	0.22	72	7	64	6	88	7
E	-42.2	2.89	0.23	71	7	66	6	86	7
ML	-42.5	3.81	0.49	70	4	64	3	86	3
EL	-42.2	3.76	0.53	68	7	59	6	88	6

Table 1 contd.

FEATURE[a]	LATITUDE (DEG.)	AIR MASS AM	ERROR	PERCENT ABSORPTION AND ERROR (Δ) FOR					
				NH_3[b]	Δ	NH_3[c]	Δ	CH_4[d]	Δ
SPR,CM	-59.2	3.59	0.21	78	5	72	4	90	5
GRS	-21.2	2.11	0.05	57	6	50	6	75	6
	-20.3	2.12	0.08	54	9	48	9	70	9
	-22.2	2.44	0.23	51	4	48	2	66	4
	-22.1	2.12	0.05	51	4	46	3	66	3
	-21.9	2.17	0.10	51	4	45	3	68	3
	-21.9	3.31	0.59	42	8	34	8	69	8
	-20.5	2.44	0.24	50	3	43	2	70	2
	-19.9	2.11	0.06	53	7	46	3	70	7
	-19.1	2.57	0.34	51	8	46	8	65	9
	-20.6	2.12	0.09	53	3	46	2	72	2
LWO 's	-31.5	2.29	0.12	70	7	64	6	82	6
	-31.4	2.39	0.18	72	5	66	4	84	4
	-31.3	3.05	0.53	67	5	60	4	83	4
	-31.9	2.55	0.23	70	4	63	2	86	3
	-31.4	2.31	0.11	69	4	62	2	82	2
	-31.2	2.59	0.24	68	4	62	2	83	2

a. The letters CM, M, L, ML, or EL following the abbreviations for the features indicate that the measurement was made at the central meridian, 1/2 between the CM and the morning limb, 1/2 between the CM and the evening limb, at the morning limb or at the evening limb respectively.
b. NH_3 absorption as determined from the data derived from the 1.47, 1.50, and 1.53 μm pass band cells.
c. NH_3 absorption as determined from the data derived from the 1.50 and 1.53 μm pass band cells.
d. CH_4 absorption as determined from the data derived from the 1.43 and 1.47 μm pass band cells.
e. questionable value

Figures 3a and 3b give the percent absorption of NH_3 (as determined by the two different sets of computation) as a function of AM for those points lying along the CM, i.e., along a N-S trace. It is apparent from Figures 3a and 3b that a) the only difference between the two sets of data is that the percent absorption as determined from all 3 cells is about 1.1 times as great as that determined by only 2 cells. Thus, the overlapping CH_4 band at 1.47 μm has no important differential effect on the data, and so only the percent absorption as determined from all 3 cells will be discussed henceforth; b) at least for the dark features (NEB, STB, NPR and SPR) the percent absorption increases with increasing air mass (AM) by a factor of 1.35 between 2 AM and 4 AM and the curve does not follow an $(AM)^{\frac{1}{2}}$ curve as would be the case for these strong bands if a simple "reflecting layer at a constant altitude" model were correct; c) the absorption over the STrZ, which was the brightest zone on the planet, is at least 1.20 times greater than for the belts at comparable AM; d) the EZ, which that season was visually quite dusky and therefore intermediate between the STrz and the belts in visual albedo, may have had a slightly greater (few percent) absorption than the belts and e) the NTrZ which was nearly as bright as the STrZ showed only a slight, if any, increase in NH_3 absorption as compared to the belts. These results are compatible with the observations of the absorption of the weak band of NH_3 over the belts and zones as made by Munch and Younkin (1964) and with the differences in strong band absorptions between the equator and the polar regions as observed by Moroz and Cruikshank.

Figures 4-5 show the variations of the NH_3 absorption along E-W traces, i.e., along belts, zones or following a spot across the disk. These graphs clearly show that the NH_3 absorption decreases as the limb (or terminator) is approached and

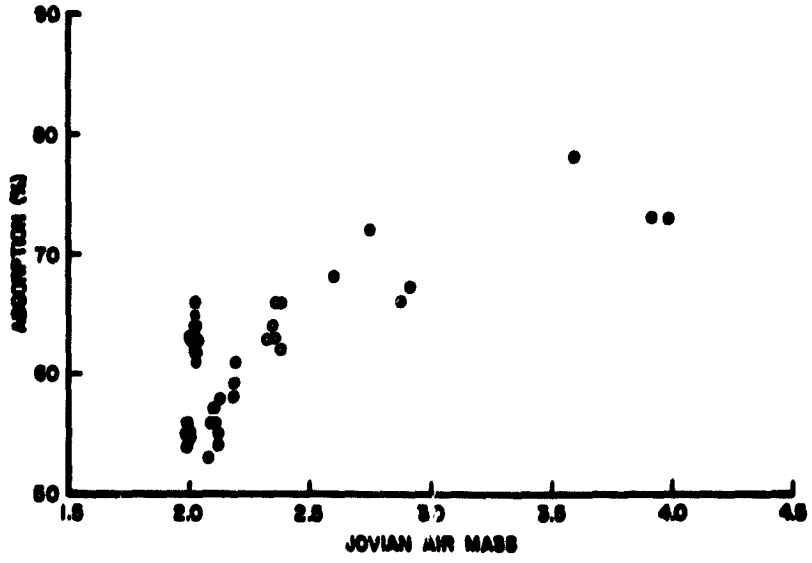

FIGURE 3a Percent absorption of NH_3 as a function of Jovian air mass for the points observed on a N-S trace along the CM. The percent absorption was computed using the data obtained from the 1.47, 1.50 and 1.53 μm passband cells (see Table 1). The filled circles represent the data for belts and polar regions. The open circles represent the data for the zones. The STrZ (at 2.05 AM) and the EZ (at 2.00 AM) lie above the curve defined by the dark features while the NTrZ (at 2.35 AM) may fall on the dark feature curve.

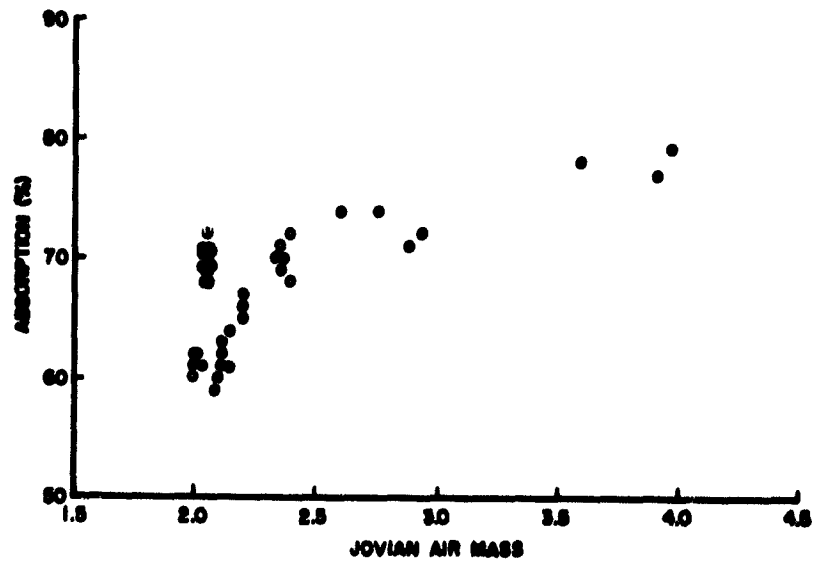

FIGURE 3b Percent absorption of NH_3 as a function of Jovian air mass for the points observed on a N-S trace along the CM. The percent absorption was computed using the data obtained from the 1.50 and 1.53 μm passband cells only (see Table 1). Otherwise, same as Figure 3a.

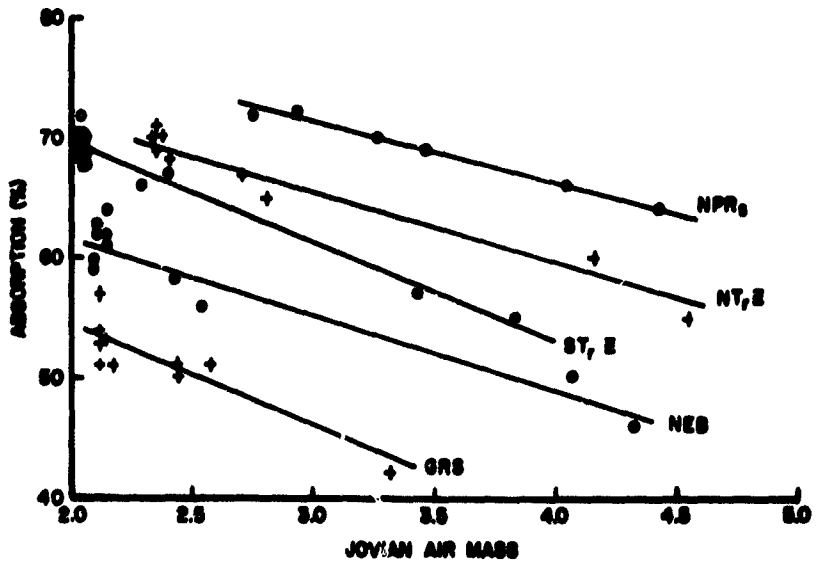

FIGURE 4 Percent absorption of NH_3 as a function of Jovian air mass for points observed along individual belts, zones, or following a spot across the disk. The percent absorption was computed using the data obtained from the 1.47, 1.50 and 1.53 μm passband cell (see Table 1).

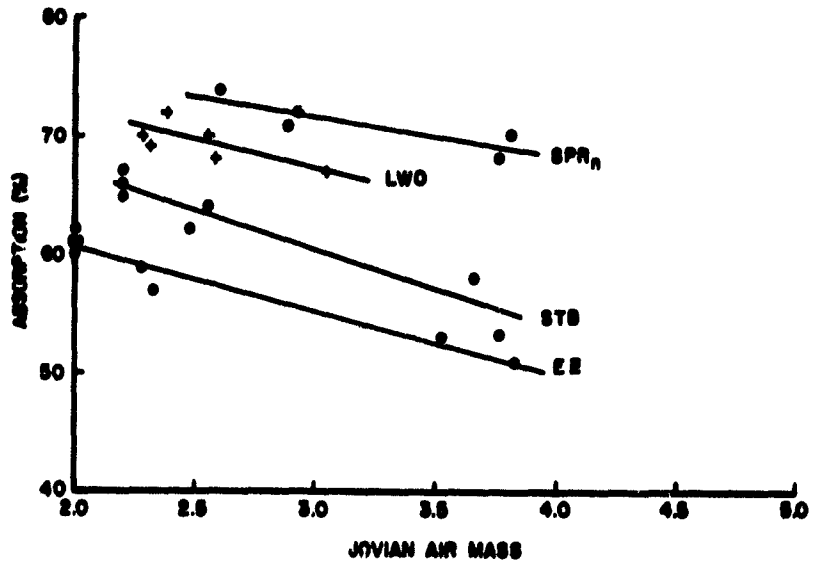

FIGURE 5 Percent absorption of NH_3 as a function of Jovian air mass for points observed along individual belts, zones, or following a spot across the disk. The percent absorption was computed using the data obtained from the 1.47, 1.50 and 1.53 μm passband cells (see Table 1).

that the decrease in absorption varies linearly, or nearly so, with air mass. Evaluation of all the E-W traces shows that within the errors of the measurements, the E-W absorption coefficient is independent of latitude and that a value of -6%/air mass gives a satisfactory fit to the data.

These E-W trace data show that the bands are being formed in a scattering atmosphere (or perhaps in an atmosphere with cumulous clouds as proposed by Squires, 1957) and thus indicate that the increase in absorption of the NH_3 with AM along the N-S trace is due to a decrease in the altitude of the scattering layer with increasing latitude or a decrease in the number of scatterers per unit column with increasing latitude.

Figure 4 also shows that the absorption over the GRS is about 0.87 times that found over the majority of the other features. This result is consistent with the finding by other investigators that the GRS lies at a higher altitude than the rest of the features. Thus at 1.5 μm and at a spatial resolution of 2".3 the only surface features which showed definite deviation from the general NH_3 absorption pattern over the disk were the STrZ and the GRS i.e., the two most prominent features on the disk.

Two effects reported by Moroz and Cruikshank, i.e., large differences in the NH_3 absorptions over the morning versus the evening limb and short time scale variations (day to day variations) of the NH_3 absorptions over particular features were not found and are presumed to be erroneous and attributable to the inherent difficulties in obtaining photometrically accurate, disk positional dependent data with a scanning spectrometer.

Since no time dependent variations were observed, the NH_3 absorption data were combined to produce an NH_3 absorption map of the planet for the months of May and June, 1970, see

Figure 6. This map clearly shows the center to limb and center to pole variation and the deep STrZ absorption. Additional belt to zone variations are strongly suggested by the contours.

3.2 THE DISTRIBUTION OF CH_4 OVER THE DISK OF JUPITER

The 1.43 and 1.47 μm cell data were used to define the percent absorption of the 1.44 and 1.47 μm CH_4 bands over the disk in the same way that the percent absorption of the NH_3 bands was determined. Because of the aforementioned overlap of the NH_3 and CH_4 bands at 1.47 μm and the near saturation of these CH_4 bands, the potential sensitivity of the measurements to detect changes in the absorption of CH_4 alone is less than for the NH_3 measurements.

Figures 7 and 8 show the percent CH_4 absorption for the N-S trace and for representative E-W traces respectively. Comparisons of these Figures with Figures 3 and 4 show that the disk position dependent variations of the CH_4 absorptions are similar to those of NH_3. The only differences being that due to the near saturation of the CH_4 bands, the percent absorption of the CH_4 is much greater than for the NH_3 and therefore that the total variation across the disk is correspondingly less. The results indicate that, for CH_4, a) the poles show only 1.20 times as much absorption as the equator, b) the STrZ absorption is 1.10 times that of the belts at equivalent AM, c) the GRS absorption is 0.90 times that of the belts, and d) the CM to limb absorption coefficient is -3%/AM, otherwise, the conclusions derived from the CH_4 absorption data are the same as those derived from the NH_3 data. Likewise, when mapped, the CH_4 absorption variations over the disk show about the same pattern as depicted in Figure 6 for NH_3.

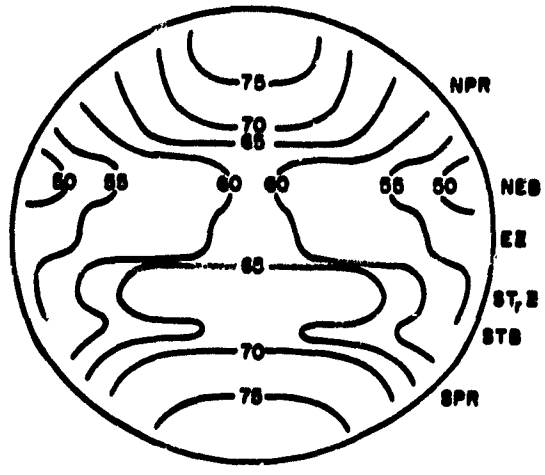

FIGURE 6 1.5 μm NH_3 absorption map for the period April - June, 1970. The contours are in percent absorption as computed using the data obtained from the 1.47, 1.50 and 1.53 μm passband cells (see Table 1).

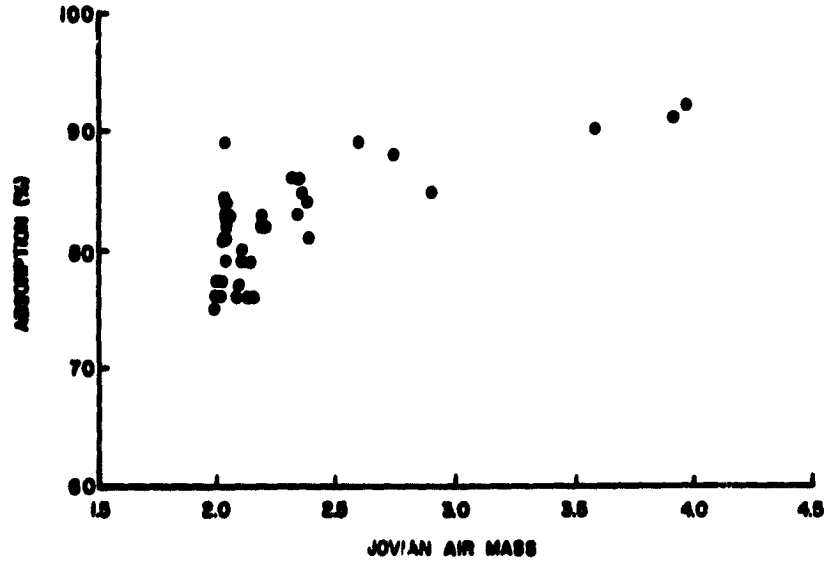

FIGURE 7 Percent absorption of CH_4 as a function of Jovian air mass for points observed on a N-S trace along the CM (see Table 1).

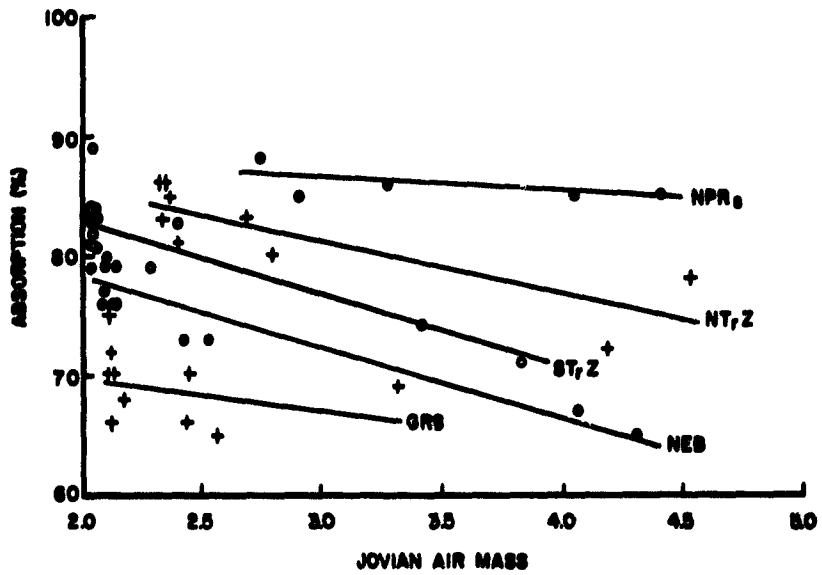

FIGURE 8 Percent absorption of CH_4 as a function of Jovian air mass for points observed along individual belts, zones or following a spot across the disk (see Table 1).

3.3 THE JOVIAN PHOTOMETRIC FUNCTION

One of the major objectives of the project was to define the photometric function of Jupiter and while, as discussed in section 2, poor weather prevented the acquisition of data over the desired wavelength range of 6000 Å to 2.3 μm, the 1.5 μm window data provided the necessary information needed to define the limb darkening in that region and thereby identify the empirical relationship which most probably can be used to define the photometric function over the full wavelength range when the data become available.

Because of the experience gained using the Minnaert function to define the Martian photometric function (as discussed in the final report on Contract NASW-2005, Binder, 1971) and because the computer subroutines were available as a result of the Mars program it was decided to attempt to use this empirical function to describe the Jovian limb darkening. The function has the form:

$$B_s = B_o \cos^k i \cos^{k-1} e$$

where B_s is the brightness of a surface element, B_o the brightness of a surface element at cos i cos e = 0, i the angle of incidence, e the angle of emission, and k a constant which describes the limb darkening. Both B_o and k are functions of the wavelength (λ) and the phase angle (α). However, the Mars program has shown that k (λ, α) does not vary rapidly with λ, and since the 1.5 μm data were taken over a small wavelength interval, little change in k (λ) would be expected. Thus, the dependence of k on λ was studied for only 2 representative wavelengths. The first wavelength (1.57 μm) was chosen because it lies nearly at the peak of the 1.5 μm window, and as a result the photometric behavior of the scattering particles or reflecting clouds could be defined as well as possible. The second

wavelength (1.47 μm) was chosen because it lies deep in the region of the NH_3 and CH_4 bands, and thus the combined effects of the absorbing gases and the particles or clouds could be defined.

Another factor to be considered in the limb darkening study is the fact that the features of Jupiter are axially symmetric, and not spherically symmetric, thus, the N-S trace data were analysed separately from the E-W trace data.

Figures 9-12 show representative plots of log (B_s cos e) versus log (cos i cos e) for N-S and E-W traces at the two chosen wavelengths. As can be seen, the data fall on sensibly straight lines as would be the case if the Minnaert function could satisfactorily describe the limb darkening of the planet.

Analysis of all the data indicates that 1) within the uncertainties of the available data, k does not show a convincing phase angle dependence; 2) the N-S trace shows that k defined within the bands is greater than the k defined near the continuum; and 3) the E-W traces show that k defined within the bands is smaller than the k defined near the continuum. Table 2 gives the values of k derived from the data.

If, as Young has suggested (private communications), an atmosphere with a thick scattering layer behaves like a Lambertian surface, i.e., $B_s = B_o$ cos i which is a degenerate form of the Minnaert function with k - 1, then the observed values of k can be explained by the observed variations of NH_3 and CH_4 over the disk as follows. At 1.57 μm, the effects of the scattering particles (or clouds) dominate the E-W traces since the amount of NH_3 absorbing in this passband is small and since, according to the NH_3 distribution data, the amount of NH_3 absorbing above the effective scattering level is constant at

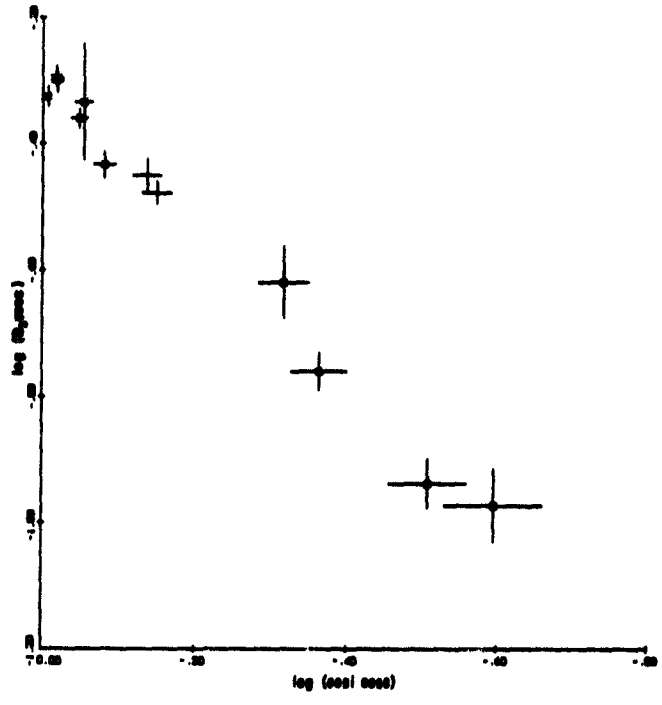

FIGURE 9 Plot of log (B_s cos e) versus log (cos i cos e) for λ=1.57 μm and α = 5°.2. The data plotted are for points observed on a N-S trace along the CM.

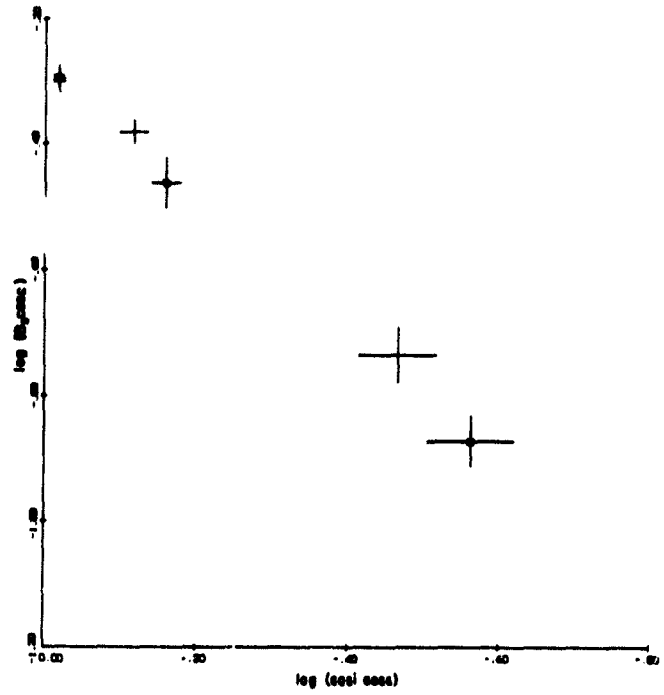

FIGURE 10 Plot of log (B_s cos e) versus log (cos i cos e) for λ = 1.57 μm and α = 5°.2. The data plotted are for points observed along the STrZ.

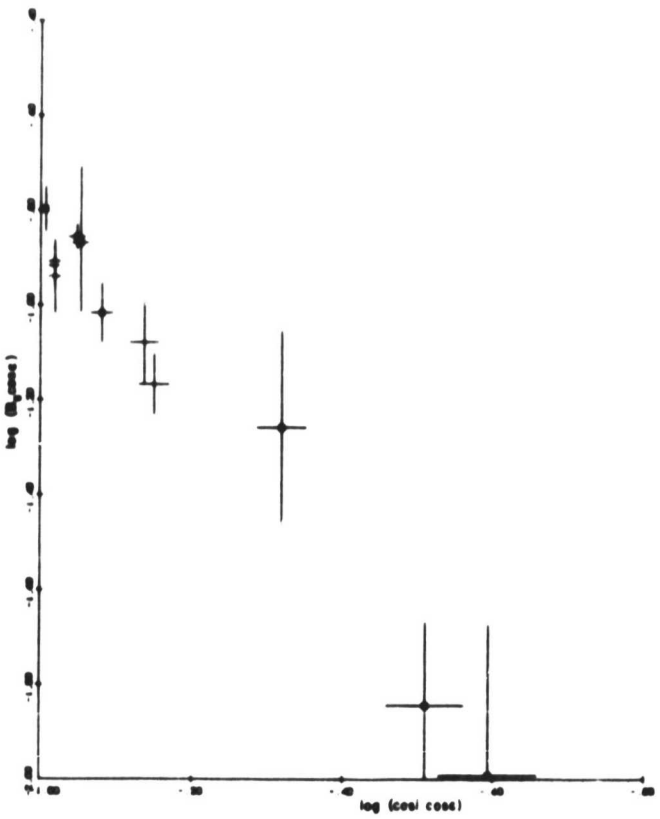

FIGURE 11 Plot of log (B_s cos e) versus log (cos i cos e) for λ = 1.47 μm and α = 5°.2. The data plotted are for points observed on a N-S trace along the CM.

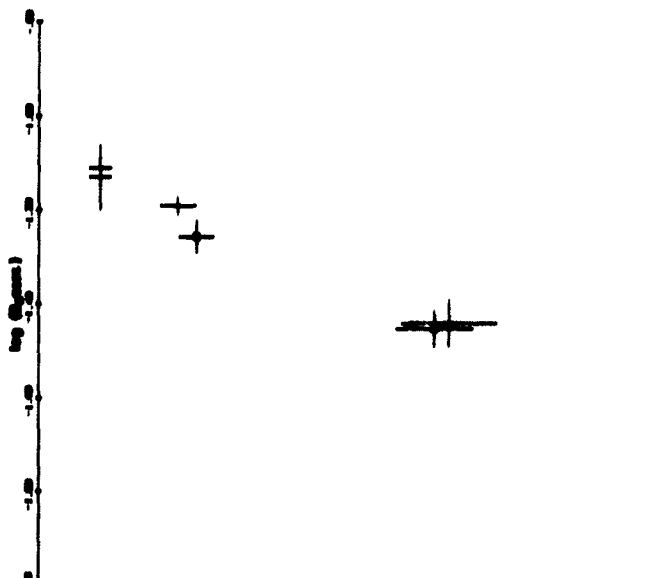

FIGURE 12 Plot of log (B_g cos e) versus log (cos i cos e) for λ = 1.47 μm and α = 5°.2. The data plotted are for points observed along the STB.

TABLE 2

LIMB DARKENING COEFFICIENTS (k) FOR JUPITER

WAVELENGTH	DIRECTION	k FOR PHASE ANGLES OF 1°.1	5°.2	9°.1
1.53 μm	N-S	1.27 ± 0.08	1.22 ± 0.06	1.5 ± .2
(near continuum)	E-W	1.0 ± 0.1	0.97 ± 0.06	———
1.47 μm	N-S	2.1 ± 0.3	2.0 ± 0.3	~ 2
(deep in NH_3 and CH_4 bands)	E-W	0.8 ± 0.2	0.7 ± 0.2	———

any particular latitude. Thus k, which would be 1 for pure scattering, is only slightly less than 1 since the limbs appear only slightly brighter than the center (i.e., when compared with pure Lambertian limb darkening) due to the slight decrease of the NH_3 absorption at the limbs. However, on the N-S trace, the NH_3 above the effective scattering level has been shown above to increase, so the N and S limbs are much darker than the center (again with respect to a Lambertian surface) and thus k will be greater than 1. At 1.47 μm, where NH_3 and CH_4 bands are very strong, the effects of the gas absorptions on the limb darkening are increased with respect to those of the scatterers or clouds. Thus, k for an E-W trace is well below 1 and k for the N-S trace is very much greater than 1.

4. THE TITAN OBSERVATIONS

As discussed in section 2, preliminary observation of the IR spectral reflectivity data for Titan were obtained under non-photometric and very poor seeing conditions. As such, the data are of low weight, but since they represent the first observation in the 10 channel spectral region, they are of interest. Figure 13 shows the relative spectral reflectivity of Titan compared to that of the center of Saturn's disk. As can be seen, the spectral reflectivity of Titan is similar to that of Saturn which most probably indicates that, like Saturn, the strong absorptions caused by the CH_4 atmosphere of Titan dominate the reflectivity curve in this region.

5. SPECTROPHOTOMETRIC DATA REDUCTION PROGRAMS

An additional result of the work done on this contract modification was that of developing data reduction programs for Jupiter/Saturn and for point or small objects such as satellites

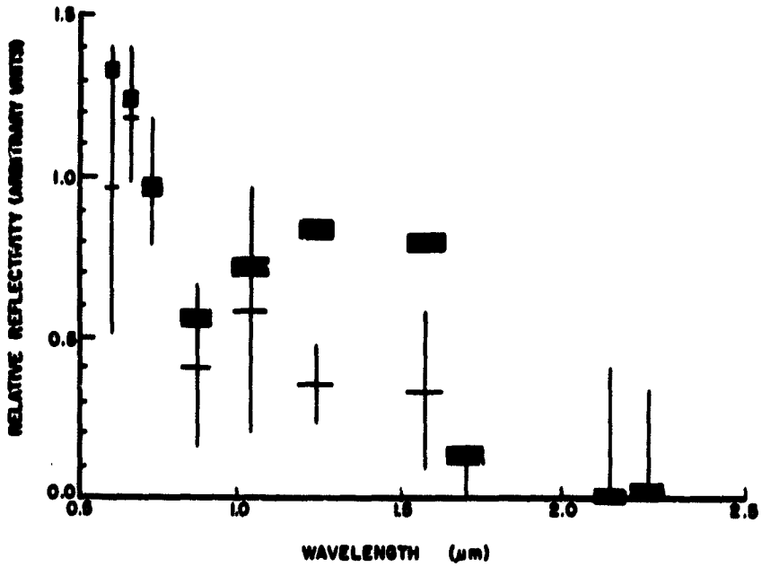

FIGURE 13 Relative reflectivity of Titan (crosses) and the center of the disk of Saturn (filled boxes) as a function of wavelength. The Titan data were normalized to the Saturn data at about 0.7 μm.

and Uranus and Neptune. The Jupiter/Saturn program (which could be easily modified to include Uranus if disk dependent data were obtained for this 4" diameter object) is similar to the Mars data reduction program described on the Final Report Contract NASW-2005(Binder,1971). However, the relatively large oblatenesses of Jupiter and Saturn precluded the use of many of the Mars program subroutines in the Jupiter/Saturn program, subroutines which compute planetocentric parameters. Thus, new subroutines were developed to compute the planetocentric latitudes, longitudes, cos i and cos e. In addition, subroutines were developed to compute the planetocentric air mass (not needed for Mars) and to determine the percent of absorption for any absorption band. As a result of this work, we now have 10 channel data reduction programs for all of the outer planets and their satellites, programs which yield normal spectral albedo data, photometric function data, atmospheric absorption data, and a number of planetocentric, astronomical, and geometric parameters which are useful in the evaluation of new types of data.

6. FUTURE WORK

Since the results of this program have demonstrated the applicability of the Minnaert function in describing the Jovian photometric function, there is a clear need for additional observational data taken over the maximum range of wavelengths and phase angles in order to define the function, as completely as possible, for both Jupiter and Saturn. Secondly, since the Minnaert coefficients are a function of the intrinsic photometric properties of the scattering particles (or clouds) in the atmosphere of Jupiter (and presumably Saturn) as well as the amount of absorbing gas above the effective scattering layer, an

effort should be made to determine if the k's vary as the bands and zones change in intensity and morphology. In this way, one may be able to detect time dependent changes in the scattering layer of the Jovian atmosphere.

Similarly, repetitive observations of the NH_3 and CH_4 absorptions over the disk at 1.5 μm would provide information on long term (and perhaps short term) time variations in the NH_3 and CH_4 distribution. Since NH_3 is a volatile in the Jovian atmosphere and, thus to a degree, it may play the same role in the Jovian atmosphere as does H_2O in the terrestrial atmosphere, NH_3 distribution maps like the one given in Figure 6, most probably will be very important in understanding Jovian meteorology.

Finally, since the attempts to obtain data on Titan, Uranus, Neptune, etc. were thwarted by observing conditions, new efforts should be made to observe these objects in order to secure the information outlined in the original proposal.

REFERENCES

Binder, A. B. (1971), Colorimetric observations of the surface of Mars, Final Report V6106, IIT Research Institute.

Cruikshank, D. P. and Binder, A. B. (1968), The Infrared Spectrum of Jupiter 0.95 - 1.60 Microns, with Laboratory Calibrations. Comm. Lunar Plan. Lab., 6, 275.

_____, (1969), Minor Constituents in the Atmosphere of Jupiter, Astrophysics and Space Science, 3, 347.

Kuiper, G. P. (1964), Infrared Spectrum of Planets and Cool Stars; Introductory Report, Memoires Soc. Roy. Sci. Liege, Cinquieme Serie, 9, 365.

Moroz, V. I. and Cruikshank, D. P., (1969), Distribution of Ammonia on Jupiter, Journal of the Atmospheric Sciences, 26, 865.

[illegible], G. and Younkin, R. L., (1964), Molecular Absorptions and Color Distributions Over Jupiter's disk, Astron. J., 69, 553.

Squires, P., (1957), The Equatorial Clouds of Jupiter, Astrophys. J., 126, 185.